10-1-2022

Intact Polar brGDGTs in Arctic Lake Catchments: Implications for Lipid Sources and Paleoclimate Applications

Jonathan H. Raberg
University of Colorado Boulder

Edgart Flores
Universidad de Concepcion

Sarah E. Crump
University of Utah, College of Mines and Earth Sciences

Greg de Wet
University of Colorado Boulder, gdewet@smith.edu

Nadia Dildar
University of Colorado Boulder

See next page for additional authors

Recommended Citation

Authors

Jonathan H. Raberg, Edgart Flores, Sarah E. Crump, Greg de Wet, Nadia Dildar, Gifford H. Miller, Áslaug Geirsdóttir, and Julio Sepúlveda

JGR Biogeosciences

Key Points:
- Intact polar branched glycerol dialkyl glycerol tetraether (brGDGT) lipids in soils were distinct from those in lakes
- In lake sediments, core brGDGTs were lacustrine in origin, and intact monoglycosyl-brGDGTs were soil derived
- Distinct intact brGDGTs could serve as proxies for both soil and lake temperatures in lake sediment archives

Correspondence to:

J. H. Raberg,
jonathan.raberg@colorado.edu

Intact Polar brGDGTs in Arctic Lake Catchments: Implications for Lipid Sources and Paleoclimate Applications

Jonathan H. Raberg[1,2], Edgart Flores[3,4,5], Sarah E. Crump[6], Greg de Wet[1,7], Nadia Dildar[1], Gifford H. Miller[1], Áslaug Geirsdóttir[2], and Julio Sepúlveda[1]

[1]Department of Geological Sciences and Institute of Arctic and Alpine Research, University of Colorado Boulder, Boulder, CO, USA, [2]Faculty of Earth Sciences, University of Iceland, Reykjavík, Iceland, [3]Programa de Postgrado en Oceanografía, Departamento de Oceanografía, Facultad de Ciencias Naturales y Oceanográficas, Universidad de Concepción, Concepción, Chile, [4]Departamento de Oceanografía, Universidad de Concepción, Concepción, Chile, [5]Millennium Institute of Oceanography, Universidad de Concepción, Concepción, Chile, [6]Department of Geology and Geophysics, University of Utah, Salt Lake City, UT, USA, [7]Now at the Department of Geosciences, Smith College, Northampton, MA, USA

Abstract Paleotemperature histories derived from lake sediment archives provide valuable context for modern and future climate changes. Branched glycerol dialkyl glycerol tetraether (brGDGT) lipids are a valuable tool in such pursuits due to their empirical correlation with temperature and near ubiquity in nature. However, the relative contributions of terrestrial and lacustrine sources of brGDGTs to lake sediments is site-dependent and difficult to constrain. Here, we explored the potential for intact brGDGTs—the complete lipids with polar head groups (HGs) still attached—to provide insight into the sources of brGDGTs on the landscape and their contributions to the sedimentary record in a set of Arctic lakes. We measured core and intact brGDGTs in soils, surface and downcore sediments, water filtrates, and sediment traps across five lake catchments in the Eastern Canadian Arctic, with an emphasis on Lake Qaupat (QPT), Baffin Island. Soils were dominated by brGDGTs with a monoglycosyl (1G) HG, while lacustrine samples contained more phosphohexose (PH) brGDGTs, providing evidence for in situ brGDGT production in both settings. Core- and PH-brGDGT-IIIa were more abundant in sediments than in the soils or water column, implying an additional post-depositional source of brGDGTs. A hierarchical clustering analysis indicated that core brGDGTs in Lake QPT sediments were largely lacustrine in origin, while 1G-brGDGTs were primarily soil-derived. Additionally, we found evidence for preservation of intact brGDGTs—especially 1G-brGDGTs—downcore on thousand-year timespans, though in situ production deeper in the sediment column cannot be ruled out. Finally, we explored the possibility of reconstructing 1G-brGDGT-derived soil temperatures and core-brGDGT-derived lake temperatures in tandem from sedimentary archives.

Plain Language Summary Bacteria can record aspects of their environment, such as temperature, via the composition of their lipid membranes. These lipids and the environmental information they contain can then be preserved in natural archives such as lake sediments, allowing for temperatures to be reconstructed deep into the past. Branched glycerol dialkyl glycerol tetraether (brGDGTs) lipids are one such type of lipid that which have become popular due to their ubiquity in nature and resistance to degradation. However, it can be challenging to figure out where the brGDGTs in a lake sedimentary archive originated. They could have been produced in the lake, washed in from surrounding soils or an inflow stream, or even been generated in the sediment itself. Here, we looked at a less commonly measured form of brGDGTs called intact polar lipids to address this question. We found that these intact lipids looked strikingly different in the soils and the lakes across five Arctic sites. We then examined one lake in further detail and found that some of the intact brGDGTs in the lake appeared to be coming from the soil. These observations could allow researchers to track changes in both soil and lake environments from lake sedimentary archives at the same time.

1. Introduction

Over the past 50 years, the Arctic has experienced substantial changes in snow cover, vegetation greening, sea and land ice cover, and precipitation (Box et al., 2019 and references within). These changes are linked in large part to a marked rise in surface air temperatures, which have been increasing at more than twice the global average for the past two decades (Ballinger et al., 2020). As high-latitude regions begin to diverge from historical analogs,

Visualization: Jonathan H. Raberg, Edgart Flores

Writing – original draft: Jonathan H. Raberg

Writing – review & editing: Jonathan H. Raberg, Edgart Flores, Sarah E. Crump, Nadia Dildar, Gifford H. Miller, Áslaug Geirsdóttir, Julio Sepúlveda

quantitative paleoclimate reconstruction becomes an increasingly important tool for constraining their possible futures (G. H. Miller et al., 2010; Tierney et al., 2020).

One tool for reconstructing high-latitude paleotemperature records is a class of bacterial cell membrane lipids called branched glycerol dialkyl glycerol tetraether lipids (brGDGTs). Structural variations in the alkyl-chain backbones of brGDGTs were found to correlate with temperature and pH in soils (Weijers et al., 2007). Analogous relationships were soon found in numerous other sample media, including lake sediments (Pearson et al., 2011; Tierney et al., 2010), allowing for the generation of global empirical temperature calibrations (Martínez-Sosa et al., 2021; Raberg et al., 2021) and the reconstruction of temperature histories from lacustrine archives across the high northern latitudes (Crump et al., 2019; Harning et al., 2020; Lindberg et al., 2021; Thomas et al., 2018).

Despite their widespread application, however, the sources of brGDGT lipids in sedimentary archives remain difficult to constrain. The seemingly ubiquitous compounds have been found in terrestrial, freshwater, and marine environments around the world (Raberg, Miller, et al., 2022). BrGDGTs in these different environments may record substantially different temperatures and can contribute to sedimentary archives to varying degrees. For example, studies that tracked the abundance and distribution of brGDGTs in lakes (De Jonge et al., 2015; Loomis et al., 2014; Tierney et al., 2012) and river systems (De Jonge et al., 2014; Guo et al., 2020; Hanna et al., 2016) have shown significant freshwater production and transport within a catchment. Furthermore, evidence has been found for brGDGT production within the lake sediments themselves (Buckles et al., 2014; Tierney et al., 2012; Van Bree et al., 2020). As a result, brGDGTs in lake sediment archives can range from largely autochthonous (e.g., Loomis et al., 2014) to primarily soil-derived (e.g., Ning et al., 2019; Peterse et al., 2014). Some tools have been developed to disentangle sources of brGDGTs in marine settings (e.g., Sinninghe Damsté, 2016; Xiao et al., 2020) and even apply mixed calibrations (Dearing Crampton-Flood et al., 2018). However, while these techniques from the marine realm have recently been tested in lacustrine systems (Martin et al., 2019) and one lake-specific brGDGT has been identified (Weber et al., 2015), methods to disentangle the various sources of brGDGTs in lake sediment archives remain in their nascent stages.

A second challenge to the interpretation of brGDGT-based paleotemperature records is the convoluting influence of dissolved oxygen (DO) levels on lipid distributions. The potential influence of oxygen depletion on brGDGT distributions was recognized early in the study of lacustrine brGDGTs (Tierney et al., 2012). Its effect has since been documented in numerous lake systems (e.g., Colcord et al., 2017; Van Bree et al., 2020; Weber et al., 2018) and in culture (Chen et al., 2022; Halamka et al., 2021, 2022) and is often associated with an increasing proportion of hexamethylated brGDGTs (e.g., IIIa). As these brGDGTs are also associated with colder temperatures, anoxic conditions in lake waters have the potential to artificially lower reconstructed temperatures. Apart from intensive studies of compound-specific isotopes (Colcord et al., 2017; Weber et al., 2018), tools for circumventing or even detecting an influence of DO on paleotemperature records are in their nascent stages (Yao et al., 2020).

The vast majority of studies on brGDGTs have relied on measurements of the recalcitrant "core" skeletons of the brGDGT lipids (c-brGDGTs). However, much additional information is contained in the more diverse pool of intact polar brGDGTs (i-brGDGTs), that is, the complete lipids with polar head groups (HGs) still attached, as they exist in living cell membranes. Due to the relatively weak bonds that typically join HGs to the rest of the compound, intact lipids in the environment tend to degrade into core lipids relatively quickly after cell death, and the information they once encoded is lost. In the laboratory, this degradation is often induced chemically; i-brGDGTs have been primarily analyzed by hydrolyzing them to their core skeletons and measuring the resulting c-brGDGT distributions. This method has allowed access to a putative "living" pool of brGDGTs, which has provided much information on the production rates and locations of brGDGTs (e.g., Cao et al., 2022; Huguet et al., 2017; Zell et al., 2013), but it sacrifices the biological, biochemical, and environmental information contained in the full suite of intact lipids.

In recent years, chromatographic methods have been developed to analyze brGDGTs in their full, intact form (e.g., Wörmer et al., 2013), though their application in the literature is limited (Liu et al., 2010; Peterse et al., 2011). These techniques expand the number of measurable brGDGTs from 15 traditional compounds to over 60, allowing for the resolution of more subtle distinctions between brGDGT distributions. Studies employing these methods have provided evidence for enhanced productivity of brGDGTs in anoxic zones of peats (Liu et al., 2010; Peterse et al., 2011). However, the distributions of i-brGDGTs across the terrestrial landscape and in lacustrine systems remain largely unexplored, and to our knowledge, no study has yet examined them in the Arctic.
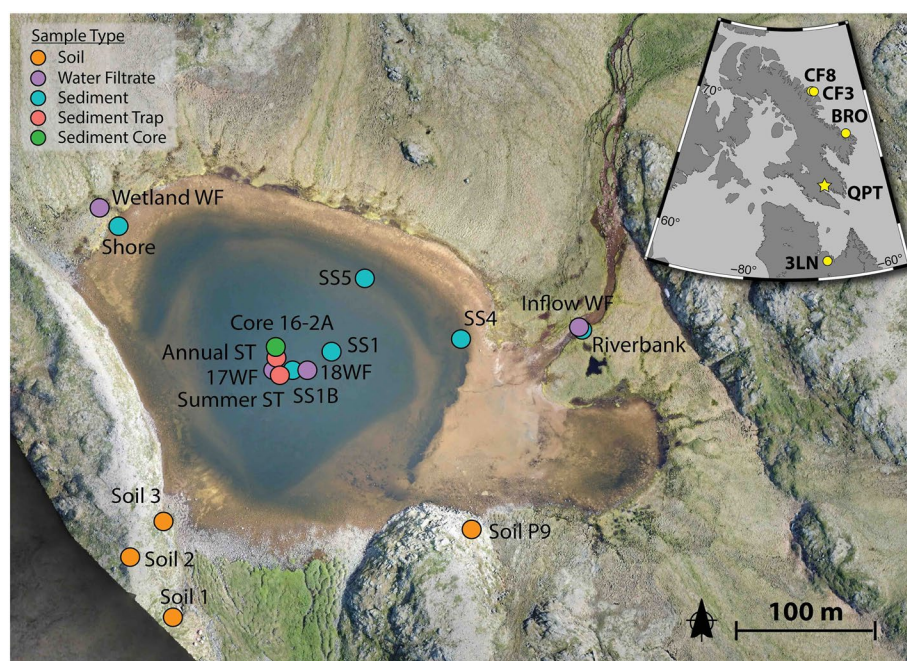
Figure 1. Drone imagery (July 2018) and sampling locations for Lake Qaupat, Baffin Island. Other sites in this study are marked in the inset: Clyde Forelands Lake 8; Clyde Forelands Lake 3; Brother of Fog Lake; and 3 Lakes North. Sample type abbreviations are as follows: surface sediment (SS), sediment trap (ST), and water filtrate (WF).

Here, we investigate the potential for i-brGDGTs to distinguish between sources of brGDGTs on the landscape in modern lake catchments from the Eastern Canadian Arctic, with an emphasis on Baffin Island. We measure brGDGTs in both their core and intact forms in soils, surface and downcore lake sediments, and aqueous environments across five lake sites, with a primary focus on Lake Qaupat (QPT). We further explore whether our findings can be used to inform c-brGDGT applications downcore and/or develop new i-brGDGT-based proxies.

2. Materials and Methods

2.1. Study Sites and Sample Collection

Soil, water filtrate (WF), sediment trap (ST), and surface sediment (SS) samples were collected from five lakes across Baffin Island, informally known as Clyde Forelands Lake 8 (CF8), Clyde Forelands Lake 3 (CF3), Brother of Fog Lake (BRO), and Lake QPT, and one lake in northern Québec (3 Lakes North (3LN)) during the summers of 2017 and 2018 (Figure 1 inset). Additionally, three samples from sediment core QPT-2A, collected in 2016 and described by Crump et al. (2019) and Gorbey et al. (2021), were re-extracted for this study, as well as downcore sediment from a suboxic interval of Early Holocene sediment collected from BRO Lake in 2017. We analyzed 55 samples in total for c- and i-brGDGTs, including 27 samples from our primary study site, Lake QPT (Figure 1).

Soils were sampled from beneath the dominant plant communities in the lake catchment (Martha K. Raynolds, personal communication in the field) at a depth interval of 0–10 cm, except for one (QPT P9), which was point sampled at 10 cm. Surface (0 m) and bottom (1–2 m above lakebed) waters were collected from lake centers and filtered through 0.3 µm glass fiber filters (Advantec). Sediment traps at deep (1.4 m above the lakebed) and shallow (2.2 m below the surface) positions at Lake QPT were deployed from August 2017 to July 2018 (ST Upper and ST Lower). After collection, these sediment traps were redeployed for the peak summer month, mid-July 2018–mid-August 2018 (ST Upper Sum and ST Lower Sum). A deep ST was also deployed from May 2018 to August 2018 at BRO Lake. Temperature, pH, conductivity, and DO concentration of the lake water columns were measured using a multiparameter sonde (HydroLab HL4, OTT HydroMet) at the time of deployment and collection of STs (Table S1 in Supporting Information S1; Raberg et al., 2021). All lakes were well oxygenated (DO saturation ≥ 90%) in the summer (July and August) except for 3LN, which had an oxycline at ~10 m depth. Additional measurements in May at lakes CF8 and BRO revealed oxygen-deficient bottom waters to exist under the lake ice (Table S1 in Supporting Information S1), in agreement with regional trends for similar lakes (Raberg

et al., 2021). Lake water samples were also collected and analyzed for total phosphorous (TP) at the University of Colorado Boulder. These data were supplemented with values for CF3 and CF8 from Michelutti et al. (2007) and personal communication with Neal Michelutti. Drone imagery was collected at 6 cm resolution with a Mavic Pro (DJI) drone on 22 July 2018. A composite (Figure 1) was generated using Maps Made Easy (Drones Made Easy).

2.2. Lipid Extraction and Analysis

After collection, samples were kept as cool as possible in the field and frozen upon returning to Colorado. All samples were freeze-dried and extracted using a modified Bligh & Dyer (BD) extraction method (Bligh & Dyer, 1959; Raberg et al., 2021; Wörmer et al., 2013). We extracted ~1 g sediment, ~5 g soil, glass fiber filters (2.5–12 L water filtered total), and all available material from sediment traps. Samples were first vortexed and sonicated in solvent Mix A, consisting of dichloromethane (DCM):methanol (MeOH):50 mM phosphate buffer (aq., pH 7.4) [1:2:0.8, v:v:v]. After centrifugation (3,000 rpm and 10°C for 10 min), the supernatant was poured or pipetted into a glass separatory funnel. The process was performed twice with Mix A, twice with Mix B (DCM:MeOH:5% trichloroacetic acid buffer (aq., pH 2) [1:2:0.8, v:v:v]), and once with Mix C (DCM:MeOH [1:5, v:v]). Separation of aqueous and organic fractions was induced by adding equal volumes of HPLC-grade water and DCM to the separatory funnel. The organic (bottom) fraction was collected and dried under a nitrogen stream. DCM was then added to the aqueous phase, shaken, and allowed to separate to remove any residual lipids. The resulting organic fraction was then added to the extract and dried. Aliquots of the resulting total lipid extract were redissolved in 99:1 (v:v) hexane:isopropanol (c-brGDGTs) or 9:1 (v:v) DCM:MeOH (i-brGDGTs) and filtered (0.45 µm, PTFE) before analysis. Six samples were additionally extracted using a standard accelerated solvent extraction (ASE) method, as described previously (Raberg et al., 2021).

Core and intact brGDGTs were analyzed using the full scan mode of a Thermo Scientific UltiMate 3,000 high-performance liquid chromatography instrument coupled to a Q Exactive Focus Orbitrap-Quadrupole high-resolution mass spectrometer (HPLC-MS). Core brGDGTs were analyzed using a slightly modified version (Raberg et al., 2021) of the chromatographic methods of Hopmans et al. (2016). Separation of i-brGDGTs was achieved using the chromatographic conditions described by Wörmer et al. (2013) and Cantarero et al. (2020). Briefly, two mobile phases (Phase A: 0.01% formic acid and 0.01% NH_4OH in acetonitrile:DCM [75:25, v:v]; Phase B; 0.4% formic acid and 0.4% NH_4OH in MeOH:H_2O [50:50, v:v]) were combined in a gradient from 1% B to 40% B. Intact brGDGTs were ionized via electrospray ionization and identified by exact masses ($\pm$5 ppm) and retention times. Due to the lack of a suitable standard, we did not quantify absolute i-brGDGT abundances. Instead, we relied on fractional abundances (FAs) of integrated peak areas as described below.

2.3. Index Calculation and Terminology

We defined multiple FAs for our analysis of both c- and i-brGDGTs. First, we calculated the standard Full Set FAs (Raberg et al., 2021) of c-brGDGTs,

$$fx_{Full} = \frac{x}{\left(Ia + Ib + Ic + IIa + IIb + IIc + IIIa + IIIb + IIIc + IIa' + IIb' + IIc' + IIIa' + IIIb' + IIIc'\right)} \quad (1)$$

where x is the integrated peak area of any compound in the denominator. An analogous FA can unfortunately not be calculated for i-brGDGTs as it is currently unknown whether the analytical method can achieve separation of the 5- and 6-methyl isomers. We therefore calculated FAs of brGDGTs for each HG using the nine compounds that are commonly measured without isomer separation and denoted the difference with an asterisk:

$$fx\text{–HG}_{Full*} = \quad (2)$$

$$\frac{x}{(HG\text{–}Ia + HG\text{–}Ib + HG\text{–}Ic + HG\text{–}IIa_C + HG\text{–}IIb_C + HG\text{–}IIc_C + HG\text{–}IIIa_C + HG\text{–}IIIb_C + HG\text{–}IIIb_C)}$$

For each HG, x is any compound in the denominator and all penta- and hexamethylated compounds represent the combined sum of 5- and 6-methyl isomers, as denoted by the subscript "C." To isolate changes in temperature-dependent methylation number, we adapted the core brGDGT Methylation Set (Raberg et al., 2021) to define analogous Meth* Set FAs,

$$fx\text{–HG}_{Meth*} = x/(HG\text{–}Ia + HG\text{–}IIa_C + HG\text{–}IIIa_C) \quad (3)$$

again using the sums of penta- and hexamethylated compounds. We additionally calculated the MBT' index (Peterse et al., 2012) for each HG,

$$MBT'_{HG} = \frac{(HG–Ia + HG–Ib + HG–Ic)}{(HG–Ia + HG–Ib + HG–Ic + HG–IIa_C + HG–IIb_C + HG–IIc_C + HG–IIIa_C)} \quad (4)$$

Finally, we calculated FAs within the entire pool of i-brGDGTs,

$$f\,x–HG_{Full-C-IPLs} = x/\sum i–brGDGTs \quad (5)$$

and the FA of each HG,

$$f\,HG = \sum HG–brGDGTs/\sum i–brGDGTs \quad (6)$$

We also used a transfer function (Equation 12 of Loomis et al. (2012)) to calculate mean annual air temperature (MAAT) from c- and i-brGDGTs,

$$MAAT\,(°C) = 22.77 − 33.58 * f\,IIIa − 12.88 * f\,IIa − 418.53 * f\,IIc + 86.43 * f\,Ib \quad (7)$$

where FAs were calculated using Equation 2 of this publication (i.e., without the separation of 5- and 6-methyl isomers).

2.4. Statistical Methods

We used principal component analysis (PCAs), one- and two-way analyses of variance (ANOVA), and hierarchical clustering to compare similarities in brGDGT distributions. PCAs were performed using the FactoMineR package in R (Lê et al., 2008; Team R Development Core, 2021). We used Full Set FAs (Equation 1) for c-brGDGTs and Full*-IPLs Set FAs (Equation 5) for i-brGDGTs. We chose the Euclidean distance measure to produce hierarchical clustering of Full* Set FAs (Equation 2). The Unweighted Pair Group Method with Arithmetic Mean (UPGMA; average-linkage) agglomerative clustering method was used according to Ramos Emmendorfer and de Paula Canuto (2021). We calculated approximately unbiased p-values (AU) and bootstrap probability values (BP). The bootstrap supports were based on 10,000 replicates and clusters with AU ≥ 95% confidence were highlighted for this study (Suzuki & Shimodaira, 2006).

3. Results

3.1. Source-Dependent i-brGDGT Distributions

BrGDGTs were detected both as core and intact polar lipids with monoglycosyl (1G) or phosphohexose (PH) HGs (Figure 2). We used a chromatographic method capable of separating the 5- and 6-methyl brGDGT isomers (solid and dashed colored methylations in Figure 2a, respectively) for core brGDGTs (see Methods). The multi-faceted peaks present for many i-brGDGTs (e.g., PH-IIa; Figure 2c) suggest the existence of isomers for these compounds as well. However, as the method used for i-brGDGTs separates compounds based on their polar HGs rather than their alkyl-chain moieties, it is uncertain whether these peaks represent 5- and 6-methyl i-brGDGTs. We did not attempt to integrate these isomers separately in this study; however, they may reflect meaningful differences (e.g., different HG positions) and their existence warrants further investigation.

Both 1G- and PH-brGDGTs were detected in most samples (Figure 3). Differences in the relative proportions of these two HGs existed between sample types (Figures 3 and 4). Soils were dominated by 1G-brGDGTs at all sites, with a mean (±1 standard deviation) FA of 1G versus PH (f1G; Equation 6) of 0.89 ± 0.10 (Figures 3 and 4). Surface sediments had a significantly lower proportion of 1G-brGDGTs ($p < 0.001$; f1G = 0.34 ± 0.21) but ranged substantially across lakes (f1G = 0.20–0.68; Figures 3 and 4). Water column samples (water filtrates and sediment traps) displayed both the largest range and within-site variance (Figures 3 and 4), likely due at least in part to low lipid concentrations in the water filtrates that may have left many compounds below the detection limit. Their f1G values were significantly different from those of the soils ($p < 0.001$), but not from those of the surface sediments ($p > 0.05$).

Finally, we examined the relationship between lake water TP and the FA of PH-brGDGTs (fPH; Equation 6) in surface sediments. While we found a weak positive correlation (adjusted $R^2 = 0.39$), it was not significant ($p > 0.2$; Figure S1 in Supporting Information S1).
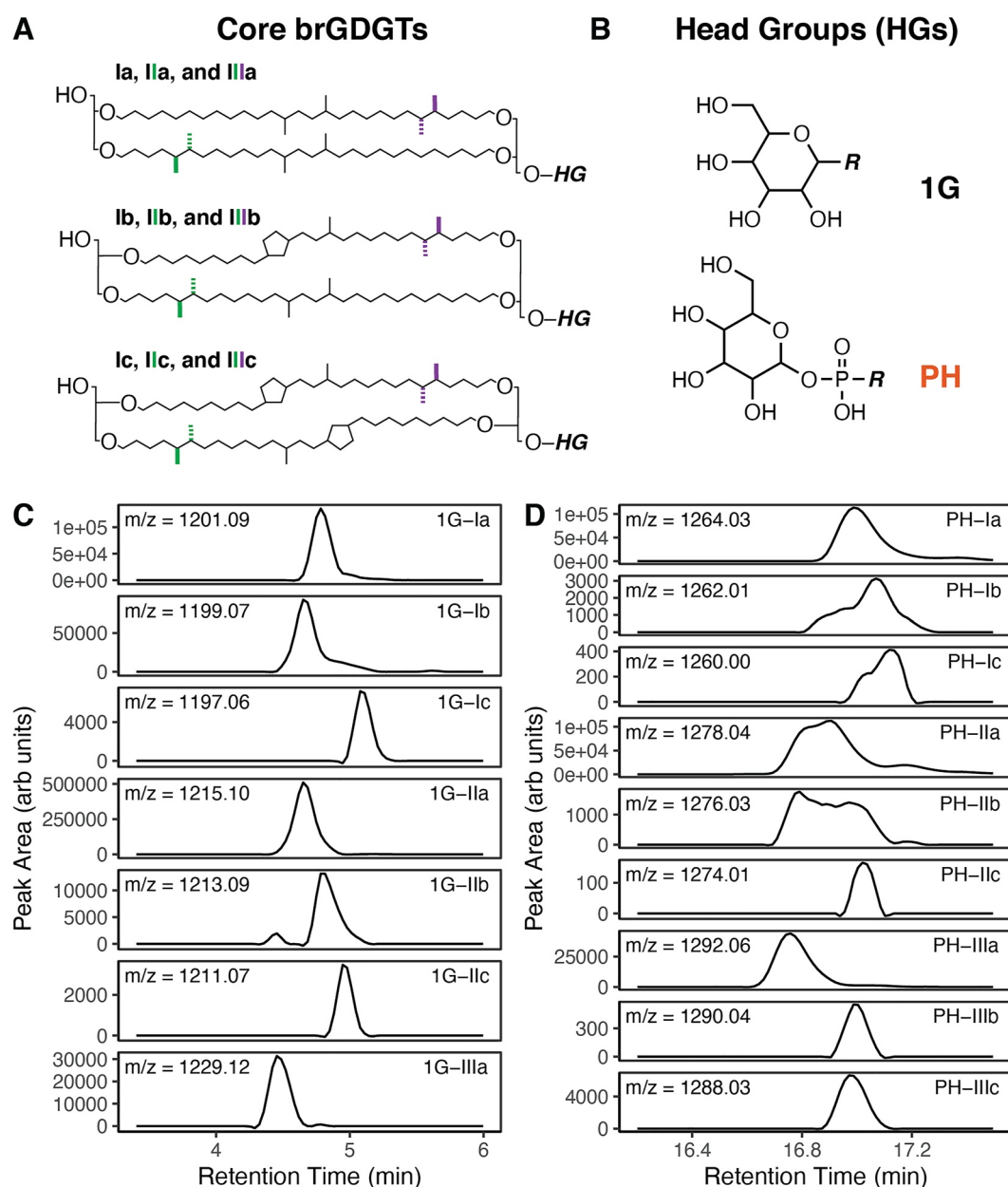
Figure 2. Structures of the (a) core branched glycerol dialkyl glycerol tetraether (brGDGTs) lipids and (b) head groups (HGs) are measured in this study. Solid and dashed lines represent methylations for the 5- and 6-methyl isomers of penta-(green) and hexa- (green + purple) methylated compounds, respectively. "*R*" denotes any core brGDGT; "HG" denotes any head group. Structures shown do not encapsulate all possible isomers. Chromatograms (smoothed, 10-point moving average) of the (c) monoglycosyl (1G)- and (d) phosphohexose-brGDGTs are shown for a representative sample (3LN Soil 2; 1G-IIIb and 1G-IIIc not detected).

3.2. Connections Between c- and i-brGDGT Distributions

To elucidate connections between c- and i-brGDGTs, we compared the distributions of brGDGTs within each group (core, 1G, and PH). We first examined regional trends using ANOVA analyses on the full data set (Figure 3). 1G-brGDGT distributions were distinct from those of PH ($p < 0.01$) and core ($p \ll 0.01$) brGDGTs, while the latter two were statistically indistinguishable ($p > 0.05$). Similarly, for surface sediments alone, 1G-brGDGTs differed from PH- ($p < 0.05$) and core ($p < 0.01$) brGDGTs but were similar to one another ($p > 0.05$). For all other sample types (soils, water filtrates, and sediment traps), the distributions of the three brGDGT types were indistinguishable ($p > 0.05$).
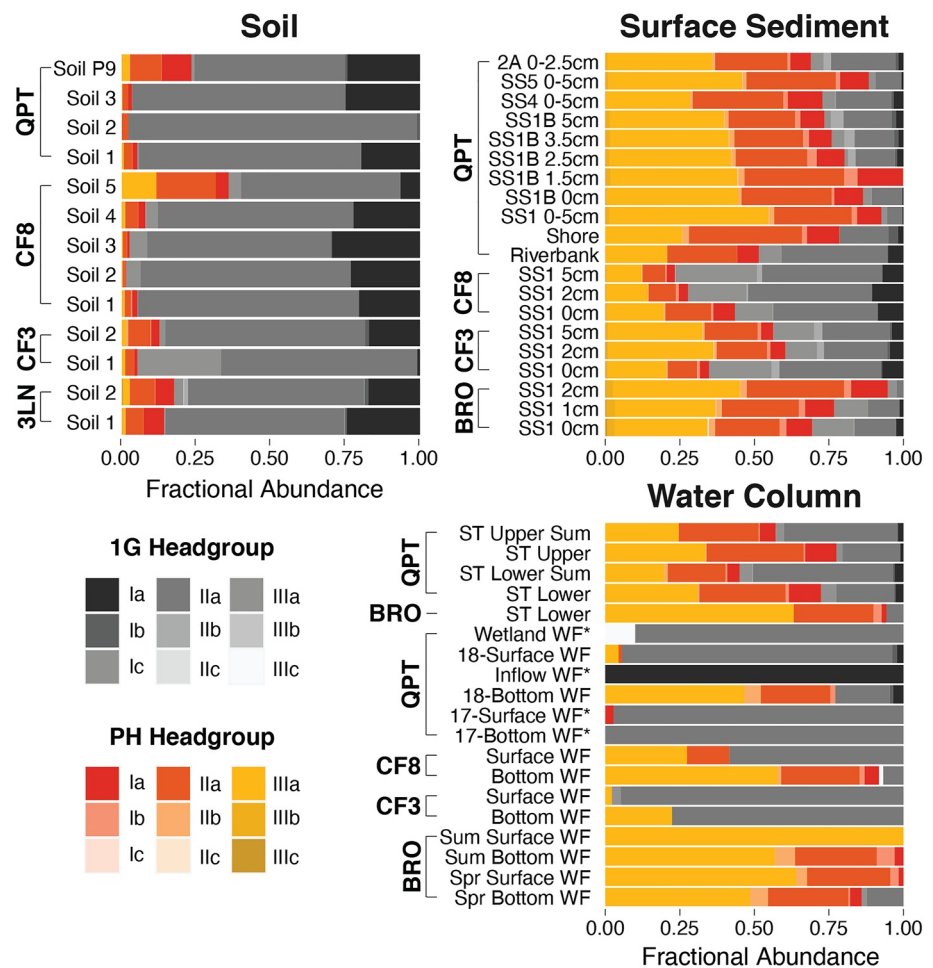
Figure 3. Fractional abundances (calculated using Equation 5 of the main text) of monoglycosyl- and phosphohexose-brGDGTs in Canadian soil, surface sediment, sediment trap, and water filtrate samples. Lake Qaupat samples marked with an asterisk were excluded from principal component and clustering analyses due to low compound abundances.

We next compared c- and i-brGDGTs at Lake QPT alone, for which we had the most comprehensive sample set (Figure S2 in Supporting Information S1). We performed PCAs on the resulting c- and i-brGDGT FAs (Equations 1 and 2; Figures 5a and 5b, respectively). In the c-brGDGT PCA, uncyclized compounds (Ia, IIa/IIa', and
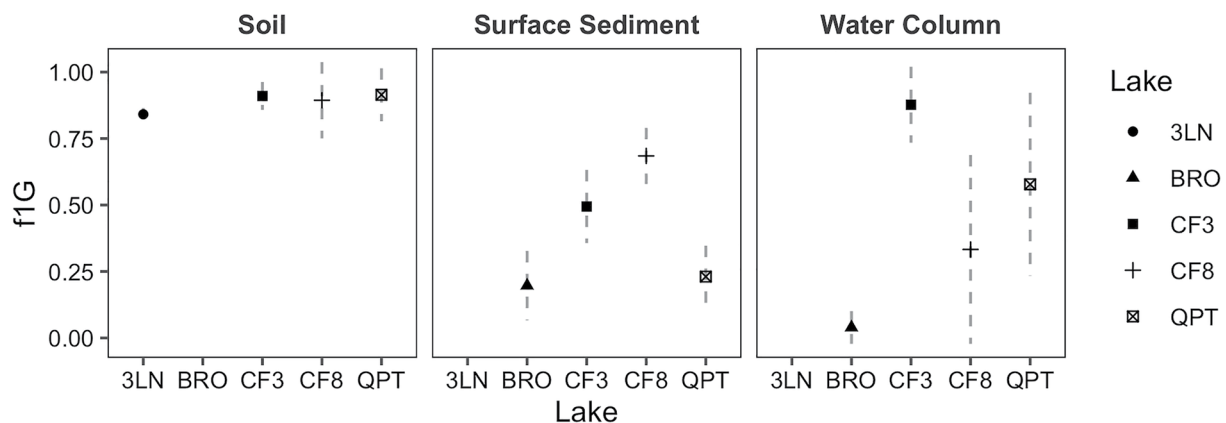

Figure 4. Mean fraction of the monoglycosyl head group by sample type. "Water Column" samples consist of sediment traps and lacustrine water filtrates. Dashed lines represent 1 standard deviation.
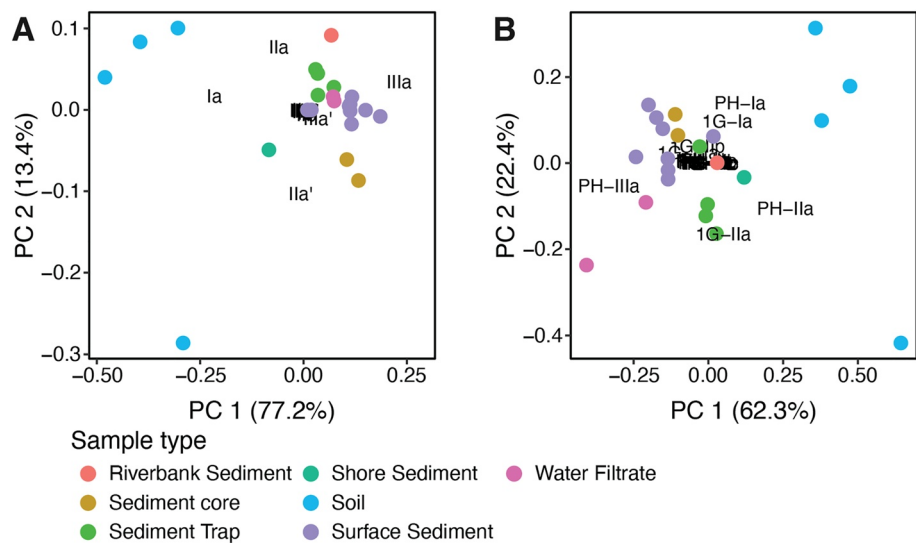
Figure 5. Principal component analyses of fractional abundances (FAs) of Lake Qaupat (a) core and (b) intact branched glycerol dialkyl glycerol tetraether (brGDGTs) lipids. FAs of c-brGDGTs were calculated according to Equation 1 (i.e., with 5- and 6-methyl isomers separated); those of i-brGDGTs were calculated with Equation 2. Compound loadings are plotted in black text (scaled by 1.8 for clarity).

IIIa) were the primary drivers of principal components 1 and 2 (PC1 and PC2), which explained a combined 90.6% of the variance and separated soils from lacustrine samples (Figure 5a). Uncyclized i-brGDGTs (especially PH-IIIa, 1G-IIa, PH-IIa, and PH-Ia) drove a similar separation of these sample types (Figure 5b). In the c-brGDGT PCA, lake surface sediments were separated from water column samples by a heightened proportion of brGDGT-IIIa (Figure 5a). Surface sediments were separated in a similar manner from sediment traps, but not water filtrates, by PH-IIIa in the i-brGDGT PCA (Figure 5b). As suggested by the c- and i-brGDGT PCAs, the Meth* Set FAs of brGDGTs IIIa and PH-IIIa displayed a strong one-to-one correlation (adjusted $R^2 = 0.80$, $p << 0.01$) across all sites and sample types, including soils (Figure 6a). In contrast, the analogous FAs of IIIa and 1G-IIIa were only weakly related (Figure 6b, adjusted $R^2 = 0.27$, and $p = 0.0003$).
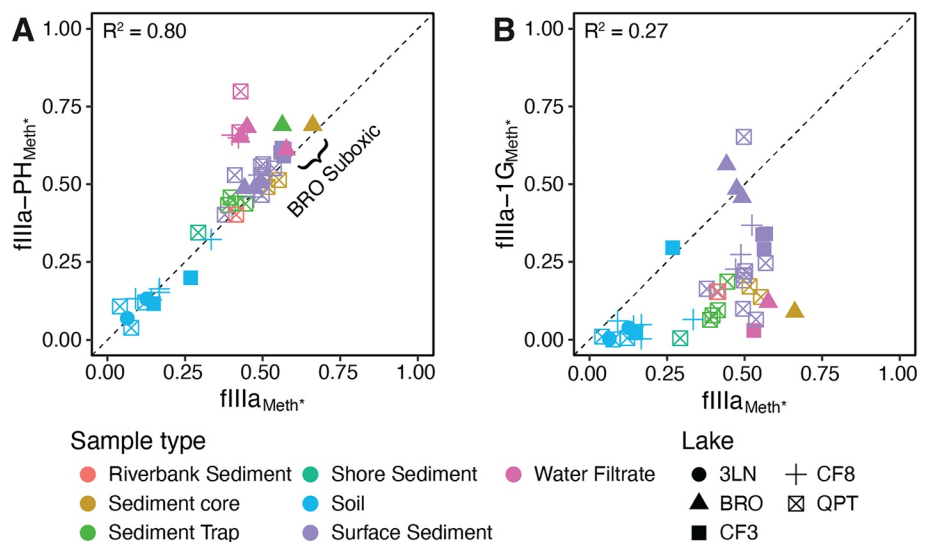

Figure 6. Relationship between the fractional abundance (FA) of IIIa in the Meth* Set (Equation 3) for the core (x-axes) and (a) phosphohexose- and (b) monoglycosyl-branched glycerol dialkyl glycerol tetraether lipids. Samples with FA = 0 or 1 were excluded. A one-to-one relationship is plotted with a dashed line. The three samples influenced by suboxic conditions (Brother of Fog Lake Spr. Bottom water filtrate, Lower sediment trap, and Early Holocene downcore sediment) are marked in panel (a). Adjusted R^2 values are provided for each plot; p-values were <0.01 for both.
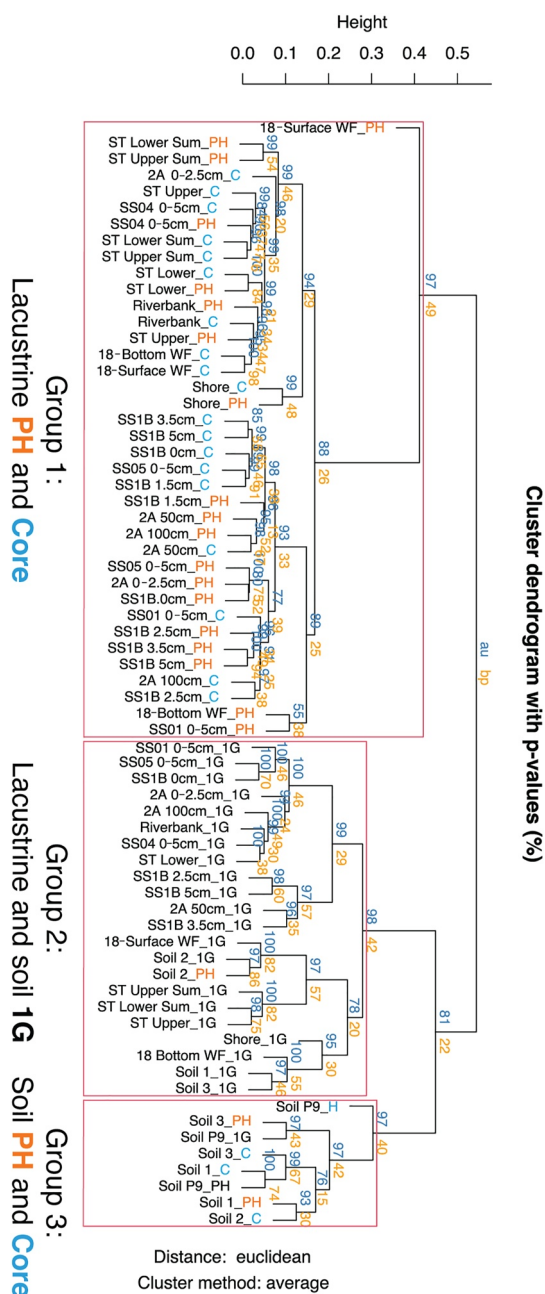
Figure 7. Clustering dendrogram of all samples at Qaupat. Fractional abundances of core lipid backbones were calculated independently for each group (core [C], phosphohexose, and monoglycosyl) accord to Equation 5. Approximately unbiased *p*-values (au; blue) and bootstrap probability values (bp; orange) are provided. Clusters with AU ≥ 95% confidence are highlighted in red boxes.

To further compare the similarities of c- and i-brGDGT distributions at Lake QPT, we performed a hierarchical cluster analysis, again using FAs calculated within each group (core, 1G, and PH) independently (Equations 1 and 2). The analysis produced three statistically significant groupings (red boxes in Figure 7; see Methods). Group 1 clustered all lacustrine core (light blue) and PH (orange) brGDGTs. Group 2 contained all 1G-brGDGT (black) distributions, including soils and lacustrine samples. Group 3 was comprised of soil core and PH distributions. Groups 2 and 3 were more similar to each other than to Group 1.

3.3. Potential for Downcore Applications

In addition to using i-brGDGTs to distinguish lipid sources in modern lake catchments, we examined their potential for applications in sedimentary archives. To test the preservation potential of i-brGDGTs, we extracted three downcore samples from Lake QPT (0, 50, and 100 cm; ~0, 4.3, and 6.3 ka (Crump et al., 2019)) and one from BRO Lake (~50–60 cm, Early Holocene in age) using the BD extraction method. Both 1G- and PH-brGDGTs were detected in all four samples (Figure 8a). However, downcore sediments are generally extracted using the ASE rather than the BD method. We therefore extracted six samples in parallel with the ASE and BD methods. We found both 1G- and PH- HGs in the BD-extracted samples, but only 1G after extracting with ASE (Figure 8b).

To test whether i-brGDGTs could serve as proxies for environmental conditions in the same manner as c-brGDGTs, we calculated MBT′ (Equation 4), the FA of IIIa in the Meth* Set (fIIIa$_{Meth*}$; Equation 3), and MAAT using a transfer function (Equation 7) from Loomis et al. (2012) from c- and i-brGDGTs at Lake QPT. For soils, the core, PH-, and 1G-brGDGTs produced statistically indistinguishable values for all three parameters ($p > 0.05$ for all combinations; Figure 9). In contrast, the three brGDGT types differed in lacustrine samples. For both fIIIa$_{Meth*}$ (Figure 9b) and MAAT (Figure 9c), for example, lacustrine core and PH-brGDGTs were distinct from 1G-brGDGTs ($p << 0.01$ for all), but were indistinguishable from one another ($p > 0.05$). For the MBT′ index, on the other hand, 1G- and PH-brGDGTs were in agreement ($p > 0.05$) while core-derived values differed from both ($p < 0.01$ for PH vs. core; $p << 0.01$ for 1G vs. core). Finally, for both MBT′ and MAAT, lacustrine 1G-brGDGTs matched soil 1G-brGDGTs ($p > 0.05$), though the two groups were distinct in fIIIa$_{Meth*}$ ($p << 0.01$). Temperatures reconstructed using two other published transfer functions (Foster et al., 2016; Pearson et al., 2011) showed greater variability among HGs (not shown).

4. Discussion

4.1. Intact brGDGTs as a Tool for Distinguishing Lipid Sources

An analysis of c- and i-brGDGT distributions revealed in situ production of brGDGTs in the soil, water column, and SS at Lake QPT. Soils were distinguished from lacustrine samples by a stark difference in the relative abundances of 1G-brGDGTs (Figures 3 and 4). Within the lake, surface sediments were further distinguished from water column samples by a heightened relative abundance of hexamethylated brGDGTs, particularly IIIa and PH-IIIa (Figures 5 and 6). These results support the conclusions of previous work using core lipids, which suggested that the production of brGDGTs is commonplace in both terrestrial and lacustrine environments (e.g., Buckles et al., 2014; Guo et al., 2020; Loomis et al., 2014; Peterse et al., 2014; Tierney et al., 2012; Weber et al., 2015).
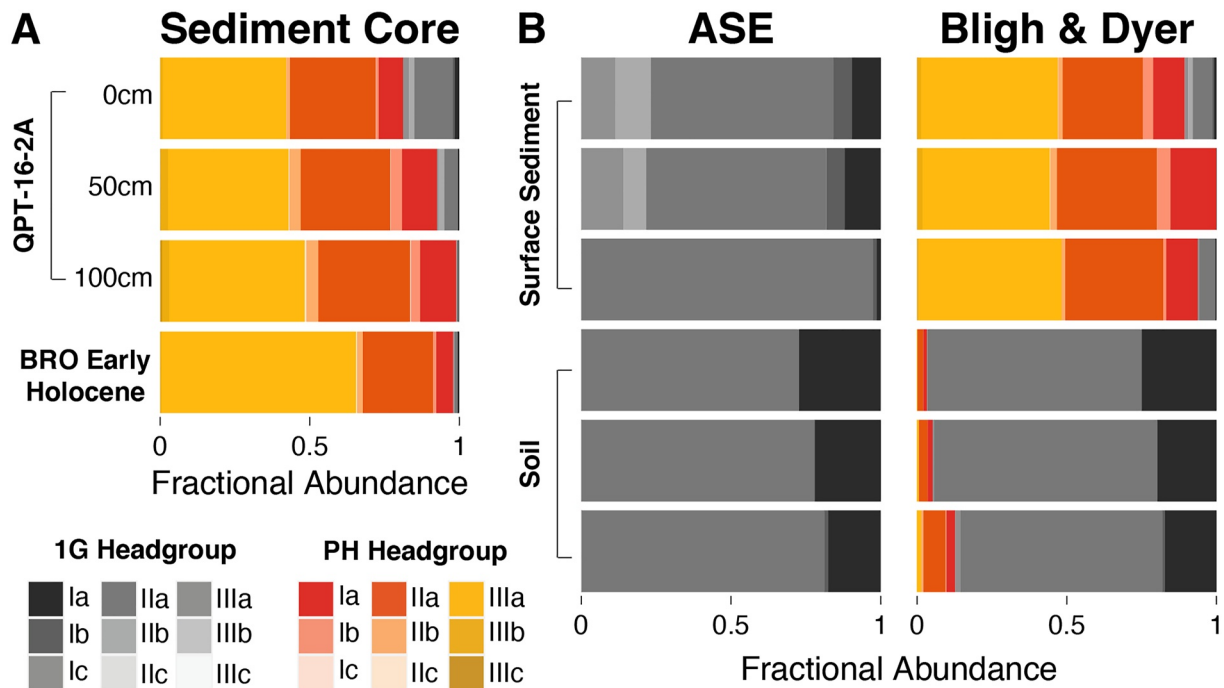
Figure 8. Potential for downcore applications of intact branched glycerol dialkyl glycerol tetraether (brGDGTs) lipids. (a) monoglycosyl- and phosphohexose-brGDGTs present in downcore sediments extracted using the Bligh and Dyer (BD) method. (b) Samples extracted in parallel using the accelerated solvent extraction and BD methods. From top to bottom, surface sediments in panel (b) are Qaupat (QPT)-SS1B 2.5, 1.5, and 0 cm and soils are QPT Soil 3, QPT Soil 1, and CF3 Soil 2 (see also Figure 3).

Widespread production poses a challenge for downcore applications, where a mixture of brGDGTs derived from multiple sources can complicate interpretations (c.f., Blaga et al., 2010). Promisingly, our results from Lake QPT suggest that 1G-brGDGTs in lacustrine samples may be primarily soil-derived and may therefore serve as a tool for detecting lipid sources at some sites. Soils at Lake QPT (and across the Canadian Arctic) were characterized by high f1G values (Figures 3 and 4). Furthermore, 1G-brGDGTs in lacustrine samples were found to have similar distributions to those in the soils, grouping together in a cluster analysis (Figure 7). These patterns suggest either that lacustrine 1G-brGDGTs are largely soil-derived or that 1G-brGDGTs are produced in similar distributions regardless of environmental setting. The fact that the cluster of 1G-brGDGTs (Group 2) is more similar
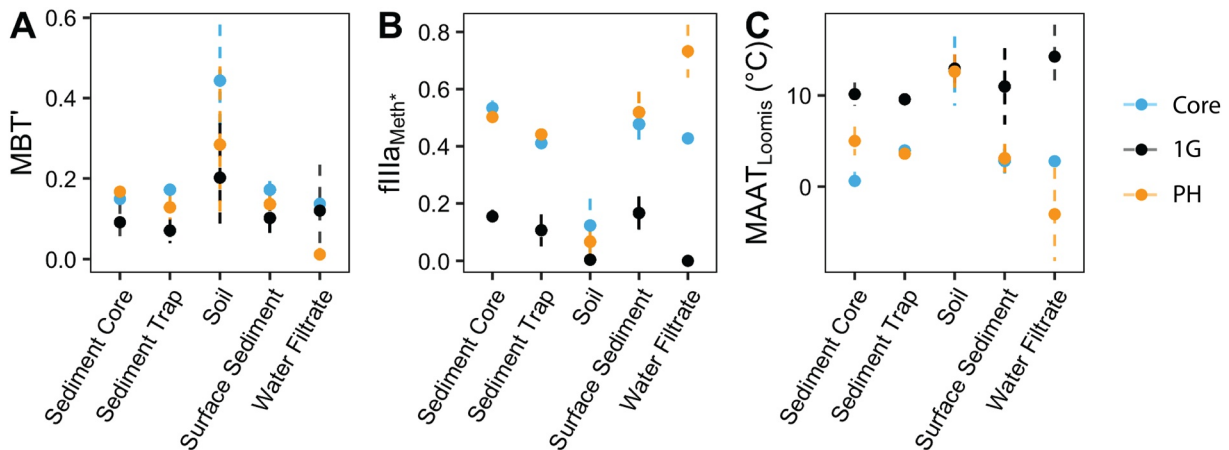

Figure 9. Mean (±1 standard deviation) of (a) the MBT' index, (b) the fractional abundance of IIIa in the Meth* structural set (Equation 3), and (c) mean annual air temperature calculated using Equation 12 of Loomis et al. (2012) for each sample type at Lake Qaupat. "Sediment Core" consists of the QPT16-2A 50 and 100 cm samples.

to soil (Group 3) than lacustrine (Group 1) core and PH-brGDGTs provides evidence for the former (Figure 7), though the latter cannot be ruled out. Finally, it is important to note that while the 1G-brGDGT distributions group together in the Lake QPT cluster analysis, different results may emerge with a larger sample set or at other lake sites. For example, surface sediments at Lakes CF3, CF8, and BRO displayed higher relative abundances of 1G-IIIa than almost all soils in this study (Figures 3 and 6b). While it is possible that soils with distributions similar to CF3 Soil 1 (Figures 3 and 6b) contribute an outsized proportion of 1G-brGDGTs to these lakes, it seems likely that at least some of the 1G-brGDGTs were produced in the lacustrine environment at these sites, perhaps driven by lower available phosphorous, which has been shown to lead to HG remodeling in other bacterial lipids (Figure S1 in Supporting Information S1; Van Mooy et al., 2009). Despite these unknowns in other lake systems, our detailed study at Lake QPT suggests that 1G-brGDGTs throughout the Lake QPT study site are primarily soil-derived.

Despite the presence of soil-derived 1G-brGDGTs in lacustrine samples, our results suggest that the fossil lipid pool is primarily derived from PH-brGDGTs produced in the lake. A cluster analysis grouped lacustrine core and PH-brGDGTs separately from soil and 1G-brGDGTs at Lake QPT (Figure 7). Furthermore, the MBT' index, fIIIa$_{Meth*}$, and MAAT$_{Loomis}$ of core brGDGTs agreed better with those derived from PH-brGDGTs than 1G-brGDGTs (Figure 9; Table S2 in Supporting Information S1). Finally, the strong correlation between the Meth* Set FAs of IIIa and PH-IIIa (Figure 6) suggests that the phospho—rather than glycolipid, may be the primary precursor of the core brGDGT-IIIa. This last connection is of particular interest for two reasons. First, a heightened relative abundance of core brGDGT-IIIa was the distinguishing marker of in situ SS production at Lake QPT. This same heightened abundance in near-surface sediments has been observed at multiple lake sites (e.g., Peterse et al., 2014; Tierney et al., 2012) and identified as the cause of an unexpected "core-top cooling" signal in paleotemperature reconstructions in which brGDGT-based temperatures decreased while instrumental records showed warming (e.g., D. R. Miller et al., 2018; Zhao et al., 2021). Second, an increased proportion of IIIa has been linked to low oxygen conditions (Loomis et al., 2011; Weber et al., 2018; Wu et al., 2021; Yao et al., 2020), causing artificially cold reconstructed temperatures in a similar manner. Samples from suboxic environments at BRO contained a heightened abundance of IIIa, in agreement with these studies, as well as a proportionally heightened abundance of PH-IIIa (Figure 6a). The tight correlation between IIIa and PH-IIIa in our study therefore suggests that the "cooling" signals in lake surface sediments and low oxygen environments may be driven by the production of hexamethylated PH-brGDGTs. We urge caution, however, in generalizing these results to other sites, as the effects of oxygen limitation on environmental brGDGT distributions are currently not well understood. While the link between IIIa and low DO has been demonstrated in some studies, for example, others have found O_2 depletion to influence other brGDGTs (e.g., Martínez-Sosa & Tierney, 2019; Van Bree et al., 2020) or to have little effect on any of them (e.g., Loomis et al., 2014).

Interestingly, the connection between core and PH-brGDGTs was apparent even for soils, despite their high f1G values. One possible explanation for the stronger relationship between PH- and c-brGDGTs is the higher lability of the PH HG (Harvey et al., 1986; Logemann et al., 2011), which could lead to a greater turnover rate and a disproportionate contribution to the fossil lipid pool. Under this hypothesis, distributions of PH-brGDGTs may respond more rapidly to changes in environmental conditions and could prove useful in studies of shorter-term (e.g., seasonal) trends in brGDGTs.

4.2. Potential Applications of i-brGDGTs in Sedimentary Archives

Both PH- and 1G-brGDGTs were detected in sediments up to 1 m below the lake floor and Early Holocene in age (Figure 8a). While these compounds represent the first i-brGDGTs measured in their intact forms downcore to our knowledge, IPL-derived c-brGDGTs have been studied in lake sediment archives (e.g., Tierney et al., 2012) and marine sediments >140 ka old (Lengger et al., 2013). Whether these downcore i-brGDGTs are produced in situ, preserved over geologic timescales, or a combination of both is not clear. Some studies have found evidence for in situ production of intact branched (Lengger et al., 2013) and isoprenoidal (Liu et al., 2011) GDGTs in marine sediments. However, these IPLs have also demonstrated a remarkable recalcitrance. Tetraethers with phosphate-based HGs have been shown to survive over millennial timescales in marine sediments (Lengger et al., 2014). Glycosidic GDGTs are even more recalcitrant, with a degradation rate on the order of millions of years (Lengger et al., 2014). Furthermore, both br- (Figure 8b; this study) and iso- (Lengger et al., 2012) GDGTs with 1G HGs have been shown to survive the high temperatures and pressures of ASE extractions. Finally, soil-derived 1G-brGDGTs appear to survive transport, deposition, and burial without significant alteration to

their distributions at Lake QPT (Figure 7). Therefore, while further study is needed to determine whether a significant in situ contribution exists, it is likely that the pool of downcore i-brGDGTs—and especially 1G-brGDGTs—at Lake QPT is predominantly ancient in origin.

The preservation of uniquely soil-derived 1G-brGDGTs into the geologic record could open the door for the development of qualitatively new proxies. BrGDGTs in lacustrine systems have been increasingly shown to be influenced by lake water chemistry, especially DO (e.g., Weber et al., 2018). This influence affects brGDGT-derived temperatures and poses a major challenge for obtaining accurate paleotemperature reconstructions. Temperatures calculated from soil-derived compounds would circumvent this issue. Furthermore, as 1G-brGDGTs survive the ASE extraction process, which is commonly used for downcore sediments, samples may not need to be (re-)extracted with the more time-consuming BD method to apply 1G-brGDGT-based proxies.

To test whether i-brGDGTs display similar temperature relationships to c-brGDGTs, we calculated and compared temperatures and temperature-related indices derived from PH-, 1G-, and core brGDGTs. The MBT' index has a positive correlation with temperature (Peterse et al., 2012). At Lake QPT, we find a general agreement in the MBT values of lacustrine samples from PH-, 1G-, and c-brGDGTs and higher and more variable values in soils. However, the MBT' index relies on several compounds (e.g., IIc) that were rare or absent from our i-brGDGT distributions, perhaps due to lower compound abundances overall, and may therefore not be appropriate for use here. A better index for the context of this study is $fIIIa_{Meth*}$. This FA relies only on the three most abundant brGDGTs (Ia, IIa_C, and $IIIa_C$) and can be expected to have a robust negative relationship with temperature (Raberg et al., 2021). As shown in Figure 9b, all three values of $fIIIa_{Meth*}$ agree well in the soils, indicating that 1G- and PH-brGDGTs have similar temperature sensitivities and that the core pool may be primarily derived from these IPLs. In contrast, lacustrine samples show good agreement between core- and PH-derived values, but a strong warm bias in those recorded by the 1G-brGDGTs. Furthermore, these 1G-derived $fIIIa_{Meth*}$ values generally agree with those recorded in the soils. This discrepancy can be explained if the PH-brGDGTs in the lake are primarily autochthonous, recording lake water temperatures, while the 1G-brGDGTs are largely allochthonous and record the temperatures of catchment soils. Under this hypothesis, a single lake sediment sample can record both soil and lake water temperatures independently. Considering that both sets of IPLs can be measured downcore, these results present the potential for independent soil and lake temperature reconstructions from the same sample extracts. Indeed, temperatures calculated using the Loomis et al. (2012) calibration appear to do just this (Figure 9c). However, other calibrations (Foster et al., 2016; Pearson et al., 2011; not shown) produce qualitatively different results, despite being tailored to high latitude regions, indicating that IPL-specific calibrations are likely to be necessary for downcore applications in the future. We also note that while analysis of the relative abundances of i-brGDGTs allows for some discrimination of lipid sources in the catchment, the current lack of suitable i-brGDGT standards makes it difficult to quantify the absolute contributions of these sources to the sedimentary record, complicating paleotemperature reconstructions.

5. Conclusions

Intact brGDGTs at Lake QPT and across the Eastern Canadian Arctic provided new insight into the sources of brGDGTs in terrestrial and lacustrine environments. We found a stark distinction between the i-brGDGT composition of soils and lacustrine samples, with 1G-brGDGTs dominating in the soils and PH-brGDGTs in the lakes. We further found heightened relative abundances of IIIa and PH-IIIa in these lake sediments, suggesting post-depositional in situ production, and in suboxic environments. 1G-brGDGTs in lacustrine samples at Lake QPT were likely soil derived, showed a high preservation potential, and survived the ASE extraction procedure, opening the door for the development of soil-specific proxies that can be measured in lake sediment archives. In contrast, core brGDGTs in the lacustrine environment were primarily derived from PH-brGDGTs produced in situ at Lake QPT. A single downcore sediment sample extracted using standard ASE methods could therefore theoretically be used to reconstruct both soil and lake water temperatures at this site. However, further work is needed to support such an approach. First, i-brGDGTs should be examined in other lacustrine settings, particularly at low latitudes, to determine which of the results observed here are specific to the Eastern Canadian Arctic and which are more widespread. Additionally, temperature calibrations should be performed for the 1G and PH HGs in both soils and lacustrine settings. Finally, further methodological developments would expand the breadth of scientific questions that could be addressed in future studies. For example, the isolation of suitable intact tetraether standards would aid in quantifying the amount of soil- versus lake-derived i-brGDGTs in lake sediments,

while the structural characterization of i-brGDGT isomers (Figure 2) might reveal novel patterns in i-brGDGTs' relationships with environmental parameters or distributions on the landscape.

Data Availability Statement

Lipid abundances of c- and i-brGDGTs for all samples in this study are available at the Arctic Data Center data repository (https://doi.org/10.18739/A2D21RK72) with a Creative Commons Universal 1.0 Public Domain Dedication (Raberg, Crump, et al., 2022).

References

Ballinger, T. J., Overland, J. E., Wang, M., Bhatt, U. S., Hanna, E., Hanssen-Bauer, I., et al. (2020). Arctic report card 2020: Surface air temperature. https://doi.org/10.25923/GCW8-2Z06

Blaga, C. I., Reichart, G. J., Schouten, S., Lotter, A. F., Werne, J. P., Kosten, S., et al. (2010). Branched glycerol dialkyl glycerol tetraethers in lake sediments: Can they be used as temperature and pH proxies? *Organic Geochemistry*, *41*(11), 1225–1234. https://doi.org/10.1016/j.orggeochem.2010.07.002

Bligh, E. G., & Dyer, W. J. (1959). A rapid method of total lipid extraction and purification. *Canadian Journal of Biochemistry and Physiology*, *37*(8), 911–917. https://doi.org/10.1139/o59-099

Box, J. E., Colgan, W. T., Christensen, T. R., Schmidt, N. M., Lund, M., Parmentier, F.-J. W., et al. (2019). Key indicators of Arctic climate change: 1971–2017. *Environmental Research Letters*, *14*(4), 045010. https://doi.org/10.1088/1748-9326/AAFC1B

Buckles, L. K., Weijers, J. W. H., Verschuren, D., & Sinninghe Damsté, J. S. (2014). Sources of core and intact branched tetraether membrane lipids in the lacustrine environment: Anatomy of Lake Challa and its catchment, equatorial East Africa. *Geochimica et Cosmochimica Acta*, *140*, 106–126. https://doi.org/10.1016/j.gca.2014.04.042

Cantarero, S. I., Henríquez-Castillo, C., Dildar, N., Vargas, C. A., von Dassow, P., Cornejo-D'Ottone, M., & Sepúlveda, J. (2020). Size-fractionated contribution of microbial biomass to suspended organic matter in the eastern tropical south Pacific oxygen minimum zone. *Frontiers in Marine Science*, *7*, 745. https://doi.org/10.3389/fmars.2020.540643

Cao, J., Lian, E., Yang, S., Ge, H., Jin, X., He, J., & Jia, G. (2022). The distribution of intact polar lipid-derived branched tetraethers along a freshwater-seawater pH gradient in coastal East China Sea. *Chemical Geology*, *596*, 120808. https://doi.org/10.1016/J.CHEMGEO.2022.120808

Chen, Y., Zheng, F., Yang, H., Yang, W., Wu, R., Liu, X., et al. (2022). The production of diverse brGDGTs by an Acidobacterium allows a direct test of temperature and pH controls on their distribution [Dataset]. BioRxiv [Preprint]. https://doi.org/10.1101/2022.04.07.487437

Colcord, D. E., Pearson, A., & Brassell, S. C. (2017). Carbon isotopic composition of intact branched GDGT core lipids in Greenland lake sediments and soils. *Organic Geochemistry*, *110*, 25–32. https://doi.org/10.1016/J.ORGGEOCHEM.2017.04.008

Crump, S. E., Miller, G. H., Power, M., Sepúlveda, J., Dildar, N., Coghlan, M., & Bunce, M. (2019). Arctic shrub colonization lagged peak postglacial warmth: Molecular evidence in lake sediment from Arctic Canada. *Global Change Biology*, *25*(12), 1–13. https://doi.org/10.1111/gcb.14836

Dearing Crampton-Flood, E., Peterse, F., Munsterman, D., & Sinninghe Damsté, J. S. (2018). Using tetraether lipids archived in North Sea Basin sediments to extract North Western European Pliocene continental air temperatures. *Earth and Planetary Science Letters*, *490*, 193–205. https://doi.org/10.1016/j.epsl.2018.03.030

De Jonge, C., Stadnitskaia, A., Fedotov, A., & Sinninghe Damsté, J. S. (2015). Impact of riverine suspended particulate matter on the branched glycerol dialkyl glycerol tetraether composition of lakes: The outflow of the Selenga River in Lake Baikal (Russia). *Organic Geochemistry*, *83–84*, 241–252. https://doi.org/10.1016/j.orggeochem.2015.04.004

De Jonge, C., Stadnitskaia, A., Hopmans, E. C., Cherkashov, G., Fedotov, A., & Sinninghe Damsté, J. S. (2014). In situ produced branched glycerol dialkyl glycerol tetraethers in suspended particulate matter from the Yenisei River, Eastern Siberia. *Geochimica et Cosmochimica Acta*, *125*, 476–491. https://doi.org/10.1016/j.gca.2013.10.031

Foster, L. C., Pearson, E. J., Juggins, S., Hodgson, D. A., Saunders, K. M., Verleyen, E., & Roberts, S. J. (2016). Development of a regional glycerol dialkyl glycerol tetraether (GDGT)-temperature calibration for Antarctic and sub-Antarctic lakes. *Earth and Planetary Science Letters*, *433*, 370–379. https://doi.org/10.1016/j.epsl.2015.11.018

Gorbey, D. B., Thomas, E. K., Crump, S. E., Hollister, K. V., Raynolds, M. K., Raberg, J. H., et al. (2021). Southern Baffin Island mean annual precipitation isotopes modulated by summer and autumn moisture source changes during the past 5800 years. *Journal of Quaternary Science*, *37*(5), 967–978. https://doi.org/10.1002/jqs.3390

Guo, J., Glendell, M., Meersmans, J., Kirkels, F., Middelburg, J. J., & Peterse, F. (2020). Assessing branched tetraether lipids as tracers of soil organic carbon transport through the Carminowe Creek catchment (southwest England). *Biogeosciences*, *17*(12), 3183–3201. https://doi.org/10.5194/bg-17-3183-2020

Halamka, T. A., McFarlin, J. M., Younkin, A. D., Depoy, J., Dildar, N., & Kopf, S. H. (2021). Oxygen limitation can trigger the production of branched GDGTs in culture. *Geochemical Perspectives Letters*, *19*, 36–39. https://doi.org/10.7185/geochemlet.2132

Halamka, T. A., Raberg, J. H., McFarlin, J. M., Younkin, A. D., Mulligan, C., Liu, X.-L., & Kopf, S. H. (2022). Production of diverse brGDGTs by Acidobacterium Solibacter usitatus in response to temperature, pH, and O2 provides a culturing perspective on brGDGT proxies and biosynthesis. *Geobiology*, 1–17. https://doi.org/10.1111/GBI.12525

Hanna, A. J. M., Shanahan, T. M., & Allison, M. A. (2016). Distribution of branched GDGTs in surface sediments from the Colville River, Alaska: Implications for the MBT′/CBT paleothermometer in Arctic marine sediments. *Journal of Geophysical Research: Biogeosciences*, *121*(7), 1762–1780. https://doi.org/10.1002/2015JG003266

Harning, D. J., Curtin, L., Geirsdóttir, Á., D'Andrea, W. J., Miller, G. H., & Sepúlveda, J. (2020). Lipid biomarkers quantify Holocene summer temperature and ice cap sensitivity in Icelandic lakes. *Geophysical Research Letters*, *47*(3), 1–11. https://doi.org/10.1029/2019GL085728

Harvey, H. R., Fallon, R. D., & Patton, J. S. (1986). The effect of organic matter and oxygen on the degradation of bacterial membrane lipids in marine sediments. *Geochimica et Cosmochimica Acta*, *50*(5), 795–804. https://doi.org/10.1016/0016-7037(86)90355-8

Hopmans, E. C., Schouten, S., & Sinninghe, J. S. (2016). The effect of improved chromatography on GDGT-based palaeoproxies. *Organic Geochemistry*, *93*, 1–6. https://doi.org/10.1016/j.orggeochem.2015.12.006

Huguet, A., Meador, T. B., Laggoun-Défarge, F., Könneke, M., Wu, W., Derenne, S., & Hinrichs, K.-U. U. (2017). Production rates of bacterial tetraether lipids and fatty acids in peatland under varying oxygen concentrations. *Geochimica et Cosmochimica Acta*, *203*, 103–116. https://doi.org/10.1016/j.gca.2017.01.012

Lê, S., Josse, J., & Husson, F. (2008). FactoMineR: An R package for multivariate analysis. *Journal of Statistical Software*, *25*(1), 1–18. https://doi.org/10.1016/j.envint.2008.06.007

Lengger, S. K., Hopmans, E. C., Sinninghe Damsté, J. S., & Schouten, S. (2012). Comparison of extraction and work up techniques for analysis of core and intact polar tetraether lipids from sedimentary environments. *Organic Geochemistry*, *47*, 34–40. https://doi.org/10.1016/j.orggeochem.2012.02.009

Lengger, S. K., Hopmans, E. C., Sinninghe Damsté, J. S., & Schouten, S. (2014). Fossilization and degradation of archaeal intact polar tetraether lipids in deeply buried marine sediments (Peru Margin). *Geobiology*, *12*(3), 212–220. https://doi.org/10.1111/gbi.12081

Lengger, S. K., Kraaij, M., Tjallingii, R., Baas, M., Stuut, J. B., Hopmans, E. C., et al. (2013). Differential degradation of intact polar and core glycerol dialkyl glycerol tetraether lipids upon post-depositional oxidation. *Organic Geochemistry*, *65*, 83–93. https://doi.org/10.1016/j.orggeochem.2013.10.004

Lindberg, K., Daniels, W., Castañeda, I., & Brigham-Grette, J. (2021). Biomarker proxy records of Arctic climate change during the mid-pleistocene transition from lake El'gygytgyn (far east Russia). *Climate of the Past*, *18*(3), 559–577. https://doi.org/10.5194/cp-2021-66

Liu, X.-L., Leider, A., Gillespie, A., Gröger, J., Versteegh, G. J. M., & Hinrichs, K.-U. (2010). Identification of polar lipid precursors of the ubiquitous branched GDGT orphan lipids in a peat bog in Northern Germany. *Organic Geochemistry*, *41*(7), 653–660. https://doi.org/10.1016/j.orggeochem.2010.04.004

Liu, X.-L., Lipp, J. S., & Hinrichs, K.-U. (2011). Distribution of intact and core GDGTs in marine sediments. *Organic Geochemistry*, *42*(4), 368–375. https://doi.org/10.1016/j.orggeochem.2011.02.003

Logemann, J., Graue, J., Köster, J., Engelen, B., Rullkötter, J., & Cypionka, H. (2011). A laboratory experiment of intact polar lipid degradation in sandy sediments. *Biogeosciences*, *8*(9), 2547–2560. https://doi.org/10.5194/bg-8-2547-2011

Loomis, S. E., Russell, J. M., Heureux, A. M., D'Andrea, W. J., & Sinninghe Damsté, J. S. (2014). Seasonal variability of branched glycerol dialkyl glycerol tetraethers (brGDGTs) in a temperate lake system. *Geochimica et Cosmochimica Acta*, *144*, 173–187. https://doi.org/10.1016/j.gca.2014.08.027

Loomis, S. E., Russell, J. M., Ladd, B., Street-Perrott, F. A., & Sinninghe Damsté, J. S. (2012). Calibration and application of the branched GDGT temperature proxy on East African lake sediments. *Earth and Planetary Science Letters*, *357*(358), 277–288. https://doi.org/10.1016/j.epsl.2012.09.031

Loomis, S. E., Russell, J. M., & Sinninghe Damsté, J. S. (2011). Distributions of branched GDGTs in soils and lake sediments from western Uganda: Implications for a lacustrine paleothermometer. *Organic Geochemistry*, *42*(7), 739–751. https://doi.org/10.1016/j.orggeochem.2011.06.004

Martin, C., Ménot, G., Thouveny, N., Davtian, N., Andrieu-Ponel, V., Reille, M., & Bard, E. (2019). Impact of human activities and vegetation changes on the tetraether sources in Lake St Front (Massif Central, France). *Organic Geochemistry*, *135*, 38–52. https://doi.org/10.1016/J.ORGGEOCHEM.2019.06.005

Martínez-Sosa, P., & Tierney, J. E. (2019). Lacustrine brGDGT response to microcosm and mesocosm incubations. *Organic Geochemistry*, *127*, 12–22. https://doi.org/10.1016/J.ORGGEOCHEM.2018.10.011

Martínez-Sosa, P., Tierney, J. E., Stefanescu, I. C., Dearing Crampton-Flood, E., Shuman, B. N., & Routson, C. (2021). A global Bayesian temperature calibration for lacustrine brGDGTs. *Geochimica et Cosmochimica Acta*, *305*, 87–105. https://doi.org/10.1016/j.gca.2021.04.038

Michelutti, N., Wolfe, A. P., Briner, J. P., & Miller, G. H. (2007). Climatically controlled chemical and biological development in Arctic lakes. *Journal of Geophysical Research*, *112*(3), G03002. https://doi.org/10.1029/2006JG000396

Miller, D. R., Habicht, M. H., Keisling, B. A., Castañeda, I. S., & Bradley, R. S. (2018). A 900-year New England temperature reconstruction from in situ seasonally produced branched glycerol dialkyl glycerol tetraethers (brGDGTs). *Climate of the Past*, *14*(11), 1653–1667. https://doi.org/10.5194/cp-14-1653-2018

Miller, G. H., Alley, R. B., Brigham-Grette, J., Fitzpatrick, J. J., Polyak, L., Serreze, M. C., & White, J. W. C. (2010). Arctic amplification: Can the past constrain the future? *Quaternary Science Reviews*, *29*(15–16), 1779–1790. https://doi.org/10.1016/j.quascirev.2010.02.008

Ning, D., Zhang, E., Shulmeister, J., Chang, J., Sun, W., & Ni, Z. (2019). Holocene mean annual air temperature (MAAT) reconstruction based on branched glycerol dialkyl glycerol tetraethers from Lake Ximenglongtan, southwestern China. *Organic Geochemistry*, *133*, 65–76. https://doi.org/10.1016/j.orggeochem.2019.05.003

Pearson, E. J., Juggins, S., Talbot, H. M., Weckström, J., Rosén, P., Ryves, D. B., et al. (2011). A lacustrine GDGT-temperature calibration from the Scandinavian Arctic to Antarctic: Renewed potential for the application of GDGT-paleothermometry in lakes. *Geochimica et Cosmochimica Acta*, *75*(20), 6225–6238. https://doi.org/10.1016/j.gca.2011.07.042

Peterse, F., Hopmans, E. C., Schouten, S., Mets, A., Rijpstra, W. I. C., & Sinninghe Damsté, J. S. (2011). Identification and distribution of intact polar branched tetraether lipids in peat and soil. *Organic Geochemistry*, *42*(9), 1007–1015. https://doi.org/10.1016/j.orggeochem.2011.07.006

Peterse, F., Meer, J. V. D., Schouten, S., Weijers, J. W. H. H., Fierer, N., Jackson, R. B., et al. (2012). Revised calibration of the MBT – CBT paleotemperature proxy based on branched tetraether membrane lipids in surface soils. *Geochimica et Cosmochimica Acta*, *96*, 215–229. https://doi.org/10.1016/j.gca.2012.08.011

Peterse, F., Vonk, J. E., Holmes, R. M., Giosan, L., Zimov, N., & Eglinton, T. I. (2014). Branched glycerol dialkyl glycerol tetraethers in Arctic lake sediments: Sources and implications for paleothermometry at high latitudes. *Journal of Geophysical Research: Biogeosciences*, *119*(8), 1738–1754. https://doi.org/10.1002/2014JG002639

Raberg, J. H., Crump, S. E., de Wet, G., Dildar, N., Miller, G., Geirsdóttir, Á., & Sepúlveda, J. (2022). Relative abundances of core and intact branched glycerol dialkyl glycerol tetraethers (brGDGTs) in eastern Canadian Arctic Lake catchments 2016-2018. https://doi.org/10.18739/A2D21RK72

Raberg, J. H., Harning, D. J., Crump, S. E., De Wet, G., Blumm, A., Kopf, S., et al. (2021). Revised fractional abundances and warm-season temperatures substantially improve brGDGT calibrations in lake sediments. *Biogeosciences*, *18*(12), 3579–3603. https://doi.org/10.5194/bg-18-3579-2021

Raberg, J. H., Miller, G. H., Geirsdóttir, Á., & Sepúlveda, J. (2022). *Near-universal trends in brGDGT lipid distributions in nature*. (Vol. 8). American Association for the Advancement of Science. https://doi.org/10.1126/SCIADV.ABM7625

Ramos Emmendorfer, L., & de Paula Canuto, A. M. (2021). A generalized average linkage criterion for Hierarchical Agglomerative Clustering. *Applied Soft Computing*, *100*, 106990. https://doi.org/10.1016/J.ASOC.2020.106990

Sinninghe Damsté, J. S. (2016). Spatial heterogeneity of sources of branched tetraethers in shelf systems: The geochemistry of tetraethers in the Berau River delta (Kalimantan, Indonesia). *Geochimica et Cosmochimica Acta*, *186*, 13–31. https://doi.org/10.1016/j.gca.2016.04.033

Suzuki, R., & Shimodaira, H. (2006). Pvclust: An R package for assessing the uncertainty in hierarchical clustering. *Bioinformatics*, *22*(12), 1540–1542. https://doi.org/10.1093/bioinformatics/btl117

Team R Development Core. (2021). *R: A language and environment for statistical computing*. R Foundation for Statistical Computing. Retrieved from http://www.r-project.org/

Thomas, E. K., Castañeda, I. S., McKay, N. P., Briner, J. P., Salacup, J. M., Nguyen, K. Q., & Schweinsberg, A. D. (2018). A wetter Arctic coincident with hemispheric warming 8,000 years ago. *Geophysical Research Letters*, *45*(19), 10637–10647. https://doi.org/10.1029/2018GL079517

Tierney, J. E., Poulsen, C. J., Montañez, I. P., Bhattacharya, T., Feng, R., Ford, H. L., et al. (2020). Past climates inform our future. *Science*, *370*(6517), eaay3701. https://doi.org/10.1126/science.aay3701

Tierney, J. E., Russell, J. M., Eggermont, H., Hopmans, E. C., Verschuren, D., & Sinninghe Damsté, J. S. (2010). Environmental controls on branched tetraether lipid distributions in tropical East African lake sediments. *Geochimica et Cosmochimica Acta*, *74*(17), 4902–4918. https://doi.org/10.1016/J.GCA.2010.06.002

Tierney, J. E., Schouten, S., Pitcher, A., Hopmans, E. C., & Sinninghe Damsté, J. S. (2012). Core and intact polar glycerol dialkyl glycerol tetraethers (GDGTs) in Sand Pond, Warwick, Rhode Island (USA): Insights into the origin of lacustrine GDGTs. *Geochimica et Cosmochimica Acta*, *77*, 561–581. https://doi.org/10.1016/j.gca.2011.10.018

Van Bree, L. G. J., Peterse, F., Baxter, A. J., De Crop, W., Van Grinsven, S., Villanueva, L., et al. (2020). Seasonal variability and sources of in situ brGDGT production in a permanently stratified African crater lake. *Biogeosciences*, *17*(21), 5443–5463. https://doi.org/10.5194/bg-17-5443-2020

Van Mooy, B. A. S., Fredricks, H. F., Pedler, B. E., Dyhrman, S. T., Karl, D. M., Koblížek, M., et al. (2009). Phytoplankton in the ocean use non-phosphorus lipids in response to phosphorus scarcity. *Nature*, *458*(7234), 69–72. https://doi.org/10.1038/nature07659

Weber, Y., Damsté, J. S. S., Zopfi, J., De Jonge, C., Gilli, A., Schubert, C. J., et al. (2018). Redox-dependent niche differentiation provides evidence for multiple bacterial sources of glycerol tetraether lipids in lakes. *Proceedings of the National Academy of Sciences of the United States of America*, *115*(43), 10926–10931. https://doi.org/10.1073/pnas.1805186115

Weber, Y., De Jonge, C., Rijpstra, W. I. C., Hopmans, E. C., Stadnitskaia, A., Schubert, C. J., et al. (2015). Identification and carbon isotope composition of a novel branched GDGT isomer in lake sediments: Evidence for lacustrine branched GDGT production. *Geochimica et Cosmochimica Acta*, *154*, 118–129. https://doi.org/10.1016/j.gca.2015.01.032

Weijers, J. W. H., Schouten, S., van den Donker, J. C., Hopmans, E. C., & Damsté, J. S. S. (2007). Environmental controls on bacterial tetraether membrane lipid distribution in soils. *Geochimica et Cosmochimica Acta*, *71*(3), 703–713. https://doi.org/10.1016/j.gca.2006.10.003

Wörmer, L., Lipp, J. S., Schröder, J. M., & Hinrichs, K. U. (2013). Application of two new LC-ESI-MS methods for improved detection of intact polar lipids (IPLs) in environmental samples. *Organic Geochemistry*, *59*, 10–21. https://doi.org/10.1016/j.orggeochem.2013.03.004

Wu, J., Yang, H., Pancost, R. D., Naafs, B. D. A., Qian, S., Dang, X., et al. (2021). Variations in dissolved O_2 in a Chinese lake drive changes in microbial communities and impact sedimentary GDGT distributions. *Chemical Geology*, *579*, 120348. https://doi.org/10.1016/j.chemgeo.2021.120348

Xiao, W., Wang, Y., Liu, Y., Zhang, X., Shi, L., & Xu, Y. (2020). Predominance of hexamethylated 6-methyl branched glycerol dialkyl glycerol tetraethers in the Mariana Trench: Source and environmental implication. *Biogeosciences*, *17*(7), 2135–2148. https://doi.org/10.5194/bg-17-2135-2020

Yao, Y., Zhao, J., Vachula, R. S., Werne, J. P., Wu, J., Song, X., & Huang, Y. (2020). Correlation between the ratio of 5-methyl hexamethylated to pentamethylated branched GDGTs (HP5) and water depth reflects redox variations in stratified lakes. *Organic Geochemistry*, *147*, 104076. https://doi.org/10.1016/j.orggeochem.2020.104076

Zell, C., Kim, J.-H., Moreira-Turcq, P., Abril, G., Hopmans, E. C., Bonnet, M.-P., et al. (2013). Disentangling the origins of branched tetraether lipids and crenarchaeol in the lower Amazon River: Implications for GDGT-based proxies. *Limnology and Oceanography*, *58*(1), 343–353. https://doi.org/10.4319/LO.2013.58.1.0343

Zhao, B., Castañeda, I. S., Bradley, R. S., Salacup, J. M., de Wet, G. A., Daniels, W. C., & Schneider, T. (2021). Development of an in situ branched GDGT calibration in Lake 578, southern Greenland. *Organic Geochemistry*, *152*, 104168. https://doi.org/10.1016/j.orggeochem.2020.104168